Excitation of a single hollow waveguide mode using inhomogeneous anisotropic subwavelength structures

Yaniv Yirmiyahu, Avi Niv, Gabriel Biener, Vladimir Kleiner, and Erez Hasman

Micro and Nanooptics Laboratory, Faculty of Mechanical Engineering and Russel Berrie Nanotechnology Institute, Technion-Israel Institute of Technology, Haifa 32000, Israel
mehasman@tx.technion.ac.il

Abstract: We propose and analyze a general approach for coupling a free space uniformly polarized beam to a desired hollow waveguide mode, thus enabling a single mode operation. The required spatial polarization state manipulation is achieved by use of inhomogeneous anisotropic subwavelength structures. Demonstration is obtained by coupling a linearly polarized CO_2 laser beam at a wavelength of $10.6 \mu m$ to the TE_{01}, TM_{01}, EH_{11}, EH_{21}, and EH_{31} modes of a $300 \mu m$ diameter dielectric-coated hollow metallic waveguide. Full polarization and intensity analysis of the beam at the waveguide's inlet and outlet ports indicates a high coupling efficiency to a single waveguide mode. Finally, shaping the waveguide mode to a nearly diffraction limited linearly polarized beam and to a radially polarized vectorial vortex are also demonstrated.

References and Links

1. J. A. Harrington, *Infrared Fiber Optics and their Applications*, (SPIE Press, 2004).
2. Lord Rayleigh, "On the passage of electric waves through tubes, or the vibrations of dielectric cylinders," Phil. Mag. **43**, 125-132 (1897).
3. E. Snitzer, "Cylindrical Dielectric Waveguide Modes," J. Opt. Soc. Am. **51**, 491-498 (1961), http://www.opticsinfobase.org/abstract.cfm?URI=josa-51-5-491.
4. E.J. Marcatili and R. A. Schmeltzer, "Hollow Metallic and Dielectric Waveguides for Long Distance Optical Transmission of Lasers," Bell. Syst. Tech. J. **43**, 1783-1809 (1964).
5. M. Miyagi and S. Kawakami, "Design theory of dielectric-coated circular metallic waveguides for infrared transmission," J. Lightwave Technol. **2**, 116-126 (1984).
6. S. Johnson, M. Ibanescu, M. Skorobogatiy, O. Weisberg, T. Engeness, M. Soljacic, S. Jacobs, J. Joannopoulos, and Y. Fink, "Low-loss asymptotically single-mode propagation in large-core OmniGuide fibers," Opt. Express **9**, 748-779 (2001).
7. B. Temelkuran, S. D. Hart, G. Benoit, J. D. Joannopoulos, Y. Fink, "Wavelength-scalable hollow optical fibres with large photonic bandgaps for CO_2 laser transmission," Nature **420**, 650 (2002), http://www.nature.com/nature/journal/v420/n6916/pdf/nature01275.pdf.
8. A. Niv, G. Biener, V. Kleiner, and E. Hasman, "Manipulation of the Pancharatnam phase in vectorial vortices," Opt. Express **14**, 4208-4220 (2006).
9. J. S. Kim, C. Codemard, J. Nilsson, and J. K. Sahu, "Erbium-ytterbium co-doped hollow optical fibre laser," Electron Lett. **42**, 515 (2006).
10. O. Shapira, K. Kuriki, N. D. Orf, A. F. Abouraddy, G. Benoit, J. F. Viens, A. Rodriguez, M. Ibanescu, J. D. Joannopoulos, Y. Fink, and M. M. Brewster, "Surface-emitting fiber lasers," Opt. Express **14**, 3929-3935 (2006).
11. I. Bassett and A. Argyros, "Elimination of polarization degeneracy in round waveguides," Opt. Express **10**, 1342-1346 (2002).
12. Z. Wang, M. Dai, and J. Yin, "Atomic (or molecular) guiding using a blue-detuned doughnut mode in a hollow metallic waveguide," Opt. Express **13**, 8406-8423 (2005).
13. M. J. Renn, D. Montgomery, O. Vdovin, D. Z. Anderson, C. E. Wieman, and E. A. Cornell, "Laser-guided atoms in hollow-core optical fibers," Phys. Rev. Lett. **75**, 3253-3256 (1995), http://link.aps.org/abstract/PRL/v75/p3253.

14. C. D. Poole, J. M. Wiesenfeld, D. J. DiGiovanni, and A. M. Vengsarkar, "Optical fiber-based dispersion compensation using higher order modes near cutoff," J. Lightwave Technol. 12, 1746-1758 (1994), http://ieeexplore.ieee.org/iel1/50/7924/00337486.pdf?arnumber=337486.
15. T. Engeness, M. Ibanescu, S. Johnson, O. Weisberg, M. Skorobogatiy, S. Jacobs, and Y. Fink, "Dispersion tailoring and compensation by modal interactions in OmniGuide fibers," Opt. Express 11, 1175-1196 (2003).
16. M. Yang, H. Chen, K. J. Webb, S. Minin, S. L. Chuang, and G. R. Cueva, "Demonstration of mode conversion in an irregular waveguide," Opt. Lett. 31, 383-385 (2006), http://www.opticsinfobase.org/abstract.cfm?URI=ol-31-3-383.
17. E. Hasman, N. Davidson, and A. A. Friesem, "Heterostructure multilevel binary optics," Opt. Lett. 16, 1460-1462 (1991), http://www.opticsinfobase.org/abstract.cfm?URI=ol-16-19-1460.
18. E. Hasman and A. A. Friesem, "Analytic optimization for holographic optical elements," J. Opt. Soc. Am. A 6, 62-72 (1989), http://www.opticsinfobase.org/abstract.cfm?URI=josaa-6-1-62.
19. J. A. Davis, G. H. Evans, and I. Moreno, "Polarization-multiplexed diffractive optical elements with liquid-crystal displays," Appl. Opt. 44, 4049-4052 (2005), http://www.opticsinfobase.org/abstract.cfm?URI=ao-44-19-4049.
20. S. C. Tidwell, G. H. Kim, and W. D. Kimura, "Efficient radially polarized laser beam generation with a double interferometer," Appl. Opt. 32, 5222- (1993), http://www.opticsinfobase.org/abstract.cfm?URI=ao-32-27-5222.
21. R. Oron, S. Blit, N. Davidson, A. A. Friesem, Z. Bomzon, and E. Hasman, "The formation of laser beams with pure azimuthal or radial polarization," Appl. Phys. Lett. 77, 3322-3324 (2000), http://scitation.aip.org/journals/doc/APPLAB-ft/vol_77/iss_21/3322_1.html.
22. M. E. Marhic, and E. Garmire, "Low-order TE_{0q} operation of a CO_2 laser for transmission through circular metallic waveguides," Appl. Phys. Lett. 38, 743-745 (1981).
23. E. Hasman, G. Biener, A. Niv, and V. Kleiner, "Space-variant polarization manipulation," in *Progress in Optics*, E. Wolf ed. (Elsevier, Netherlands, Amsterdam, 2005) Vol. 47 .
24. A. Niv, G. Biener, V. Kleiner, and E. Hasman, "Propagation-invariant vectorial Bessel beams obtained by use of quantized Pancharatnam-Berry phase optical elements," Opt. Lett. 29, 238-240 (2004), http://www.opticsinfobase.org/abstract.cfm?URI=ol-29-3-238.
25. A. Niv, G. Biener, V. Kleiner, and E. Hasman, "Rotating vectorial vortices produced by space-variant subwavelength gratings," Opt. Lett. 30, 2933-2935 (2005), http://www.opticsinfobase.org/abstract.cfm?URI=ol-30-21-2933.
26. W. S. Mohammed, A. Mehta, M. Pitchumani, and E. G. Johnson, "Selective excitation of the TE_{01} mode in hollow-glass waveguide using a subwavelength grating," Photon. Technol. Lett. 17, 1441 (2005).
27. Y. Yirmiyahu, A. Niv, G. Biener, V. Kleiner, and E. Hasman, "Vectorial vortex mode transformation for a hollow waveguide using Pancharatnam-Berry phase optical elements," Opt. Lett. 31, 3252-3254 (2006), http://www.opticsinfobase.org/abstract.cfm?URI=ol-31-22-3252.
28. A. Niv, G. Biener, V. Kleiner, and E. Hasman, "Spiral phase elements obtained by use of discrete space-variant subwavelength gratings," Opt. Commun. 251, 306–314 (2005).
29. R. George and J. A. Harrington, "Infrared transmissive, hollow plastic waveguides with inner Ag-AgI coatings," Appl. Opt. 44, 6449-6455 (2005), http://www.opticsinfobase.org/abstract.cfm?URI=ao-44-30-6449.
30. V. G. Niziev and A. V. Nesterov, "Influence of beam polarization on laser cutting efficiency," J. Phys. D 32, 1455-1461 (1999).

1. Introduction

Hollow waveguides present an alternative to solid core fibers at the infra-red (IR) regime where suitable optical materials are scarce. In addition, due to their air core, they can be used for broad-spectrum high power transmission as they suffer from small insertion losses. As a result, hollow waveguides are used in industrial and medical applications involving CO_2 and Er:YAG lasers as well as for spectroscopic and radiometric measurements [1]. In 1897, Lord Rayleigh [2] was the first to consider using hollow metallic waveguides for the propagation of electromagnetic radiation. However, he considered the metal to be a perfect conductor, thus his solution is inadequate in optical regimes where metal behaves more like a lossy dielectric. In 1961, Snitzer presented a general treatment for the propagation of electromagnetic fields inside cylindrical waveguides of arbitrary material [3]. A convenient approximation for circular metallic waveguides was later presented by Marcatili and Schmeltzer in 1964 [4]. In 1984, Kawakami and Miyagi proposed an improved design in which an additional inner dielectric multilayer stack is used to reduce transmission losses [5]. Recently, a new design for a circular hollow Bragg waveguide, which is a type of photonic bandgap fiber, has been presented [6, 7]. In this case, guiding is obtained by reflection from a periodic dielectric layers rather than by metal cladding. Therefore, the waveguide performance is no longer limited by the metallic losses.

A hollow waveguide supports vectorial modes in a manner determined by its structure and material composition. It is customary to classify the modes: transverse electric-TE_{0m}, transverse magnetic-TM_{0m}, and hybrid-HE_{nm} and EH_{nm} -modes. The integers n, $m>0$ denote the azimuthal and radial mode orders [3]. The commonly used modes of circular hollow waveguides are the TE_{01} and HE_{11}; The TE_{01} is an azimuthal linearly polarized vectorial vortex having a dark central core [8]. This mode possesses the least amount of loss in a bare circular metallic hollow waveguide as well as in the circular hollow Bragg waveguide [6]; The HE_{11} mode is linearly polarized and has a bright central core. It is the lowest order mode in terms of waveguide cutoff. It is important to note that a general hollow waveguide mode has a spatially varying polarization state, with the exception of the linearly polarized HE_{1m} set of modes.

While current applications of hollow waveguides, such as power delivery, rely on multimode operation, future applications might benefit from the ability to excite only a single waveguide mode. Such applications include hollow waveguide lasers [9,10] and single TE_{01} mode circular Bragg waveguides [11]. We expect that additional applications of hollow waveguides might emerge once higher order modes are exploited. For example, the mode's dark core increment with azimuthal mode order n might prove useful for blue detuned atom guiding [12, 13]. Also higher order modes can be used for dispersion compensation [14, 15].

Coupling a single hollow waveguide mode requires matching the phase, amplitude, and polarization state. Phase and amplitude matching methods are well developed and can be achieved by conventional optical devices, irregular waveguides [16], and diffractive or holographic optics [17, 18]. However, matching the polarization state is more challenging. Several techniques for this purpose exist such as liquid crystal spatial light modulators [19], interferometric techniques [20], and lasers with intra-cavity optical devices [21, 22]. However, all these methods are either cumbersome, have low power thresholds or inadequate in the IR regime.
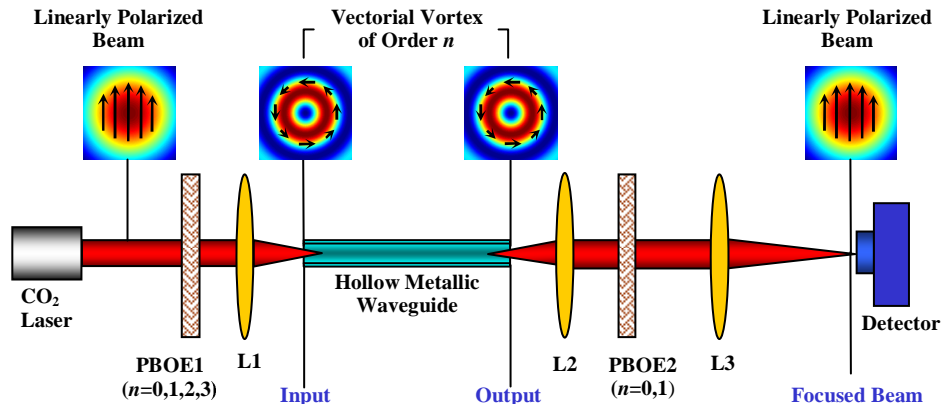
Fig. 1. (color online) Schematic representation of the experimental apparatus. Insets illustrate false color intensity distributions and polarization orientation (black arrows) of the beam at different locations along the experimental apparatus.

Recently, we have demonstrated spatial polarization state manipulation by space-variant subwavelength gratings [23]. These devices act as waveplates with space-variant orientations and as inhomogeneous anisotropic subwavelength structures, they are particularly well suited for polarization manipulation. As the optical properties of these devices stem from the geometric Pancharatnam-Berry phase, they are called Pancharatnam-Berry phase optical elements (PBOEs). PBOEs are both compact and efficient optical devices. They were used for the formation of propagation invariant vectorial Bessel beams [24], rotating vectorial vortices [25], and for the excitation of a vectorial hollow waveguide mode in the $1.55\mu m$ wavelength

regime [26]. Furthermore, we have presented the use of PBOEs for the coupling and inverse coupling of free-space linearly polarized beams to a hollow waveguide's azimuthally polarized vectorial TE$_{02}$ mode [27].

In this paper, we propose a general approach for coupling free space beams to any of the hollow waveguide modes, thus enabling single mode operation. Figure 1 shows a schematic presentation of our concept. A laser beam is coupled to a single waveguide mode by the subwavelength grating PBOE1 and the lens L1. Afterwards, the emerging beam is collimated and transformed into a free space mode using the lens L2 and PBOE2. The lens L3 is used for focusing the beam onto a two dimensional detector array. In section 2 we present the design of a PBOE for the excitation of a hollow waveguide mode using a linearly polarized laser beam, and analyze its efficiency. Section 3 focuses on the demonstration of our technique by exciting the TE$_{01}$, TM$_{01}$, EH$_{11}$, EH$_{21}$, and EH$_{31}$ modes of a hollow metallic waveguide using 10.6μm wavelength beam from a CO$_2$ laser. Validation of efficient single mode excitation is obtained by performing full polarization and intensity analysis of the beam at the waveguide's inlet and outlet. In addition, we demonstrate inverse coupling of the emergent TE$_{01}$ mode to a nearly diffraction limited linearly polarized bright spot, and to a ring-like radially polarized beam. Finally, concluding remarks are presented in section 4.

2. Theoretical background

Hollow waveguides possess a discrete set of propagating modes labeled by their radial and angular indexes m, n. The general structure of these modes is well known [3]. The mode's field distribution as well as propagation constant, loss, and dispersion can be found by solving a transcendental characteristic equation. We consider a waveguide with a core diameter much larger than the wavelength used, so that only the transverse electric part of the mode is treated. According to Miyagi and Kawakami [5], for the fundamental azimuthal dependence
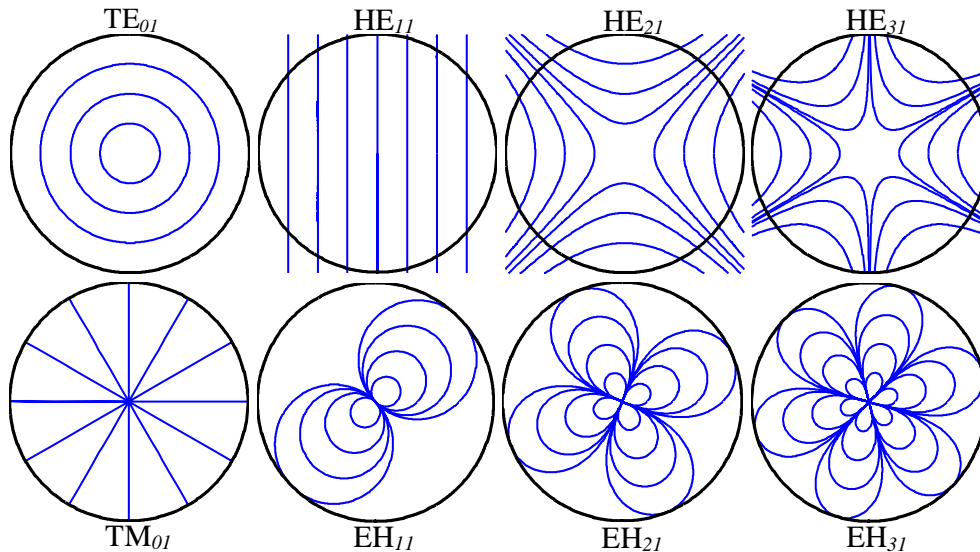
Fig. 2. Electric field lines of metallic hollow waveguide modes.

of n=0, this waveguide's modes split into separate sets: the transverse electric (TE) and transverse magnetic (TM), (see Fig. 2). The TE modes are azimuthally polarized according to,

$$\left| E_{\varphi,0m} \right\rangle = J_1\left(u_{0m} r / a\right) \left| \varphi \right\rangle , \tag{1}$$

while the TM$_{0m}$ modes are radial,

$$\left| E_{r,0m} \right\rangle = -J_1 \left(u_{0m} r / a \right) \left| r \right\rangle . \tag{2}$$

In the case $n \neq 0$, this type of waveguide supports EH_{nm} and HE_{nm} set of modes with a transverse electric field given by,

$$\left| E_{nm} \right\rangle = J_{n\mp 1} \left(u_{nm} r / a \right) \left[\pm \cos \left(n\varphi + \varphi_0 \right) \left| r \right\rangle - \sin \left(n\varphi + \varphi_0 \right) \left| \varphi \right\rangle \right], \tag{3}$$

where upper or lower signs indicate either the HE_{nm} or EH_{nm} set of modes, respectively. Here, $\left| r \right\rangle = \left[\exp(i\varphi) \left| R \right\rangle + \exp(-i\varphi) \left| L \right\rangle \right] / \sqrt{2}$ and $\left| \varphi \right\rangle = i \left[\exp(i\varphi) \left| R \right\rangle - \exp(-i\varphi) \left| L \right\rangle \right] / \sqrt{2}$ stands for radial and azimuthal polarizations with $\left| R \right\rangle = (1, -i)^T / \sqrt{2}$ and $\left| L \right\rangle = (1, i)^T / \sqrt{2}$ as right- and left-handed circular polarizations. Additionally, r and φ are the radius and azimuth polar coordinates in the transverse plane of the waveguide, a is the waveguide's air core radius, u_{nm}/a is a complex transverse phase constant, and $J_l(x)$ is the first-kind Bessel function of order l.

When the period of a dielectric grating is sufficiently smaller than the wavelength of the impinging beam, the grating behaves as a uniaxial crystal with optical axes parallel and perpendicular to the grating strips. Therefore, by controlling θ, the local orientation of the dielectric subwavelength grating, waveplates with a space-varying fast axis are achieved [23]. This enables formation of beams with almost arbitrary space-variant polarization states. We have previously shown [23] that for linearly polarized illumination, the beam that emerges from a π retardation PBOE is given by,

$$\left| E_{out,n} \right\rangle = \cos(2\theta - \varphi) \left| r \right\rangle + \sin(2\theta - \varphi) \left| \varphi \right\rangle . \tag{4}$$

Comparing this result to the waveguide's modes in Eqs. (1), (2), and (3) we find that by setting the PBOE local groove orientation to be,

$$\theta = \frac{1 \mp n}{2} \varphi + \frac{\varphi_0}{2} , \tag{5}$$
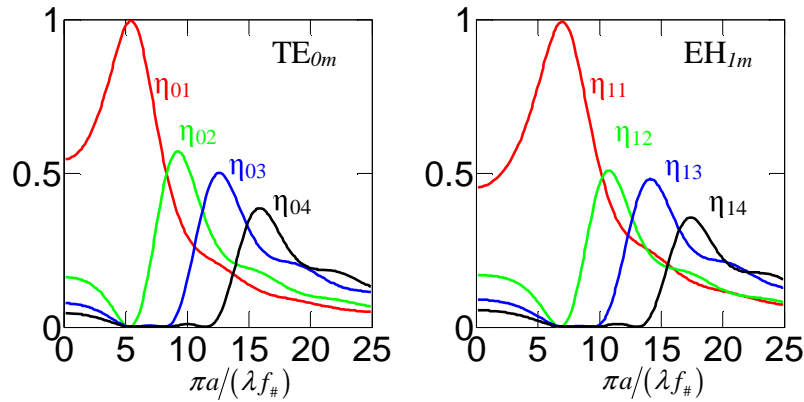
Fig. 3. (color online) Coupling coefficients for the TE_{0m} (left) and the EH_{1m} (right) sets of modes.

the polarization state of the waveguides modes, as depicted in Fig. 2, is exactly reproduced. The upper '-' and lower '+' signs correspond to the HE_{nm} and EH_{nm} set of modes, respectively. It is important to note that in order to avoid limitations imposed by the continuous groove orientation, it is approximated by a piecewise continuous orientation composed of constant orientated zones [28]. We have shown that when 16 discrete zones are used, diffraction is negligible (more than 98% to the first diffraction order, according to Ref.

(28). For a more comprehensive discussion of PBOEs, we encourage the reader to consult references 23-25, 28.

After having achieved the desired polarization state, in order to obtain an efficient coupling as well, the magnitude and phase distribution of the incident beam should also match those of the waveguide mode. We show that this can be achieved, to a satisfactory degree, by using a simple focusing lens. Immediately after the PBOE, the beam $\left| E_{out,n} \right\rangle$ has uniform intensity and the desired polarization state. By placing the PBOE at the front focal plane of a lens, we obtain at the back focal plane a field of the form,

$$\left| E_{f,n} \right\rangle = A_n(r) \left| E_{out,n} \right\rangle,$$ (6)

where,

$$A_n(r) = -\frac{i\lambda f}{2\pi r^2} \int_0^{\frac{2\pi R_0}{\lambda f} r} x J_{1 \mp n}(x) dx.$$ (7)

Here, λ is the wavelength, R_0 is the aperture radius, f is the lens focal length, and the '-' and '+' signs correspond to TE/HE and TM/EH sets of modes, respectively. The field in Eqs. (6)-(7) represents concentric intensity rings that bear a close resemblance to the hollow waveguide modes. In order to evaluate the coupling efficiencies between this field and the waveguide mode we define a coupling coefficient according to,

$$\eta_{nm} = \frac{\left| \left\langle E_{f,n} \middle| E_{nm} \right\rangle \right|^2}{\left\langle E_{f,n} \middle| E_{f,n} \right\rangle \left\langle E_{nm} \middle| E_{nm} \right\rangle}.$$ (8)

Figure 3 shows η_{nm} for the TE_{0m} and the EH_{1m} modes versus the dimensionless parameter $\pi a/(\lambda f_\#)$, ($f_\# = f/2R_0$). For example, for the TE_{0m} modes we obtain coupling efficiencies close to 1, 0.55, and 0.48 for $\pi a/(\lambda f_\#) = 5.4, 9, 12$, which corresponds to a radial mode order of $m=1$, 2, and 3, respectively. We also calculated coupling efficiencies close to unity (about 0.99) with $\pi a/(\lambda f_\#) = 3.7, 7, 8.4, 9.7$ for the HE_{11}, EH_{11}, EH_{21}, and EH_{31} modes, respectively (not shown in the figure). Therefore, it is possible to achieve high coupling coefficients for modes of radial order $m=1$ by choosing an appropriate focal length f.
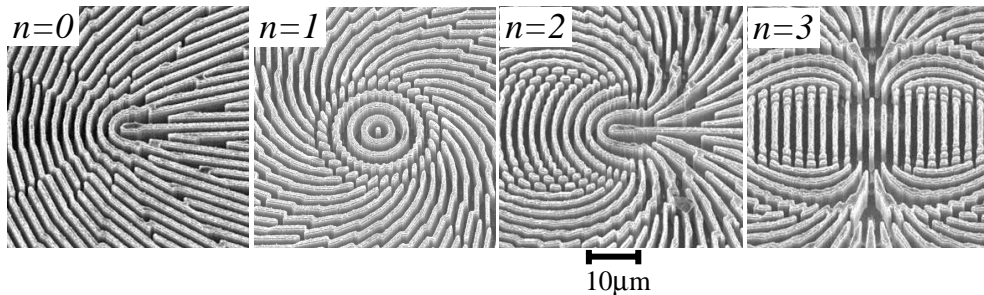
Fig. 4. Scanning Electron Microscope (SEM) images of PBOEs for coupling a linearly polarized $10.6\mu m$ wavelength beam to hollow waveguide modes of different azimuthal order n.

3. Experimental results and analysis

In order to test our approach, we used the apparatus schematically depicted in Fig. 1. A $10.6\mu m$ wavelength beam from a CO_2 laser illuminated PBOEs whose azimuthal order ranged from $n=0$ to 3. The PBOEs, $10mm$ in diameter, were realized upon GaAs wafers and had a subwavelength period of $\Lambda=2\mu m$, a fill factor of 0.5, and a nominal etching depth of $5\mu m$ so as to achieve the desired π retardation. The desired groove orientation, given by Eq.

(5), was approximated by 16 discrete zones for which we calculated diffraction efficiency greater than 98%. Figure 4 shows scanning electron microscope images of the devices. The discrete changes in the groove orientation as well as the high aspect ratio and rectangular shape of the grooves are clearly observed. The beam emerging from PBOE1, now having the correct polarization distribution, was focused onto the waveguide inlet using lens L1. The lens aperture and the focal length were adjusted to obtain optimal coupling according to Eq. (8) and Fig. 3. We used a $61cm$ commercially available Ag/AgI hollow silica waveguide with a $300\mu m$ inner bore diameter (Polymicro HWCA300750). Finally, lenses L2 and L3 together with PBOE2 were used to modify the waveguide mode to either a diffraction limited focus spot, or a radially polarized vectorial vortex. We demonstrate our approach by measuring the full polarization state at the waveguide entrance and outlet ports. The results for excitation of different waveguide modes are shown in Figs. 5-7 using the following template: The upper and lower rows relate to the waveguide's input and outlet ports, respectively. The first and second columns show false color images of the initial intensity and the intensity after a polarizer, respectively. The dashed line indicates the waveguides circumference while yellow arrows show the polarizer's orientation. The third column shows the measured local polarization ellipse's orientation. Finally, the fourth column shows a typical measured (dots) and predicted [solid line, from Eq. (7)] intensity cross-section.

Measured results for exciting the TE_{01} mode are shown in Fig. 5. The power at the waveguide inlet was measured to be $170mW$. The doughnut-shaped intensity results from the vectorial vortex induced by the PBOE. The propeller-like intensity fringes after the polarizer indicate the existence of an azimuthally polarized vectorial vortex at the waveguide entrance.
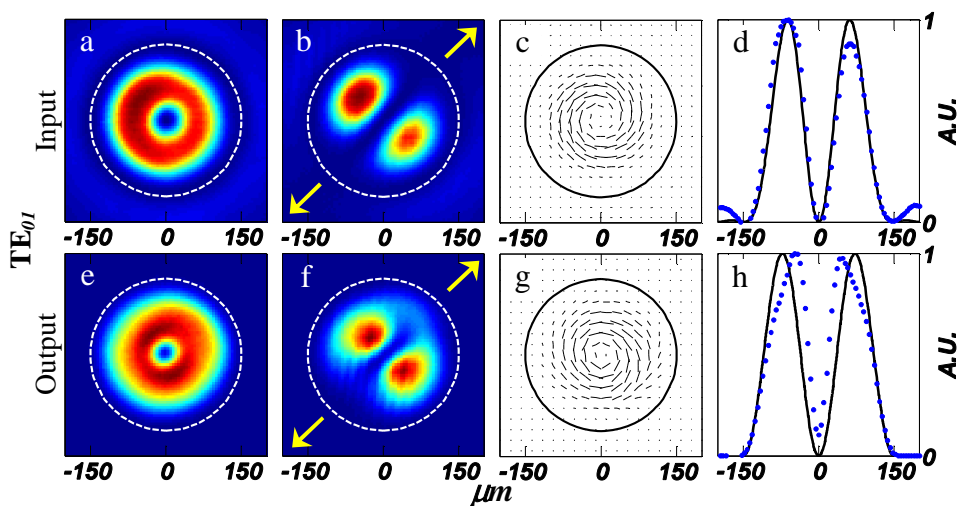
Fig. 5. (color online) Measured intensity and polarization for coupling to the TE_{01} mode at the waveguide's inlet (top) and outlet (bottom) ports. The first column depicts false color intensity representation with dashed line indicating the waveguide's inner circumference. The second column depicts false color representation of the intensity after a linear polarizer whose orientation is given by the yellow arrows. The third column shows the measured polarization ellipse's orientation, with bar length indicating intensity. The fourth column shows the measured (dots) and predicted (solid lines) intensity cross sections.

This result is supported by the polarization ellipse orientation whose typical deviation from the desired orientation, as calculated by Eq. (1), was 0.12 radians with a similar value for the mean ellipticity. Therefore, we obtained the required linearly polarized azimuthally oriented vectorial vortex at the waveguide entrance. In addition, the calculated and measured cross-sections indicate that the correct intensity profile was also achieved. At the waveguide's outlet, the single intensity ring and the evident propeller-like intensity behind the polarizer demonstrate a close resemblance to the TE_{01} mode. The deviation of the polarization

orientation from its desired value was 0.2 radians, with the ellipticity deviation less than 0.3 radians. Therefore, the field at the outlet port has the correct linear azimuthal $n=0$ polarization structure. Turning to the cross-section plot, a good agreement is found between the predicted and measured values, thereby verifying the required intensity profile of radial index $m=1$, and thus the existence of a nearly single TE_{01} mode. Variations are attributed to residual high order TE_{0m} modes from the coupling process described in section 2, and to mode mixing along the nearly straight waveguide. Comparing the measured equivalent losses (insertion + propagation) of $4.7db/m$ at the waveguide outlet to the calculated $4.13db/m$ TE_{01} mode losses [5] indicates the low insertion losses of our apparatus. Therefore, an efficient single mode excitation is demonstrated.

Figure 6 demonstrates coupling of the TM_{01} mode in much the same way as in Fig. 5. As can be seen from the measurements at the waveguide inlet, this mode differs from the TE_{01} only by the local polarization orientation, namely radial instead of azimuthal. Consequently, it is coupled using an identical PBOE of order $n=0$, while either the PBOE or the incoming beam is rotated by a right angle. The intensity and polarization measurements performed at the waveguide's inlet and outlet indicate successful coupling of this mode.

Figure 7 shows the measured intensity and polarization at the fiber inlet and outlet for the EH_{11}, EH_{21}, and EH_{31} modes. Good agreement of the results with the desired intensity distribution, polarization orientation, and cross-section indicates the ability to obtain a single high order excitation. The distortion of the high order modes at the waveguide inlet results from greater variation in the required polarization distribution. Further distortion at the waveguide outlet is attributed to mode mixing, and higher propagation losses along the waveguide (after Ref. 5: $10.25db/m$, $15.82db/m$, and $22.38db/m$ for the EH_{11}, EH_{21}, and EH_{31} modes, respectively), thus reducing the signal-to-noise ratio in these cases.
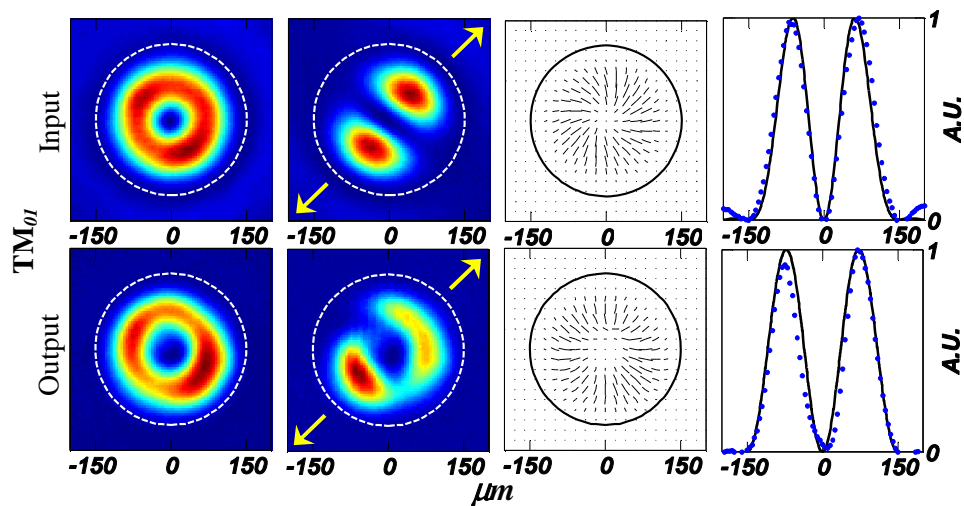
Fig. 6. (color online) Measured intensity and polarization for coupling to the TM_{01} mode at the waveguide's inlet (top) and outlet (bottom) ports. The first to fourth columns depict the intensity (dashed line indicates the waveguide inner circumference), intensity after a polarizer (arrows indicate polarizer orientation), measured polarization orientation, and intensity cross-section (dots-measured, solid line-predicted), respectively.

For many applications, manipulation of the fiber mode at the waveguide outlet is desired. An example is the transformation of a waveguide mode to a uniformly polarized free space beam so as to achieve high focusability, or to a radially polarized vectorial vortex for efficient metal cutting [30]. The required polarization manipulation can be obtained by inverting our coupling mechanism, as depicted in Fig. 1. In this case, the 1" focal length lenses L2 and L3, serve as a *4-f* system with PBOE2 placed in an intermediate focal plane. The PBOE modifies the polarization of the hollow waveguide mode to any desired polarization.
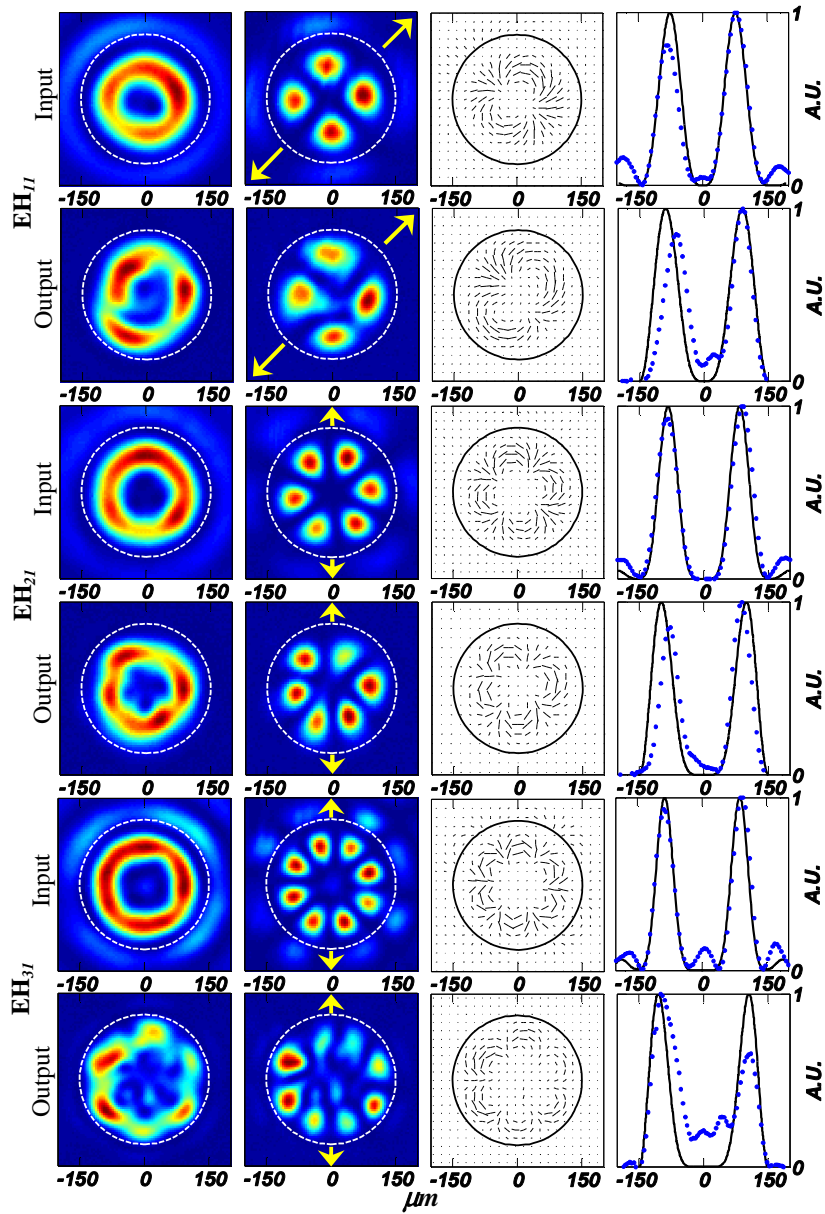
Fig. 7. (color online) Measured intensity and polarization for coupling the high order modes at the waveguide's inlet and outlet ports. The first to forth columns depict the intensity (dashed line indicates the waveguide's inner circumference), intensity after a polarizer (arrows indicate polarizer orientation), measured polarization orientation, and intensity cross-section (dots-measured, solid line-predicted), respectively.

Transforming the azimuthal polarization of the TE_{01} mode to a linear polarization can be obtained by a PBOE with $n=0$. This arises from a general property of π-retardation PBOEs, namely that $T^2=-I$ where T is the PBOE transmission matrix and I is the unit matrix. Figure 8(a) shows, in the usual manner, the measured results at the focus of the L3 lens. The absence of a distinctive doughnut intensity pattern results from the polarization manipulations of PBOE2. The focusability factor of the intensity spot was measured to be $M^2=1.7$. This is a

considerable improvement over the $M^2=2.2$ of the TE$_{01}$ mode. Furthermore, by removing the intensity side lobes, seen in the intensity cross-section, we can achieve a focusability of $M^2=1.1$ with a mere 11% intensity loss. Thus, the ability to obtain a diffraction-limited spot by using PBOEs is demonstrated. For comparison, Fig. 8(b) shows the intensity without a PBOE inserted in the intermediate focal plane of the L2 and L3 lenses. Note the larger focal spot of the azimuthal linearly polarized vectorial vortex with respect to the linearly polarized focus of Fig. 8(a). Figure 8(c) demonstrates transformation of the TE$_{01}$ waveguide mode to a radially polarized vectorial vortex by using a PBOE with $n=1$ as PBOE2. The results indicate that the desired radially polarized vectorial vortex was achieved. We therefore demonstrate the ability of a PBOE (together with lenses) to efficiently couple a waveguide mode to a desired free-space mode.
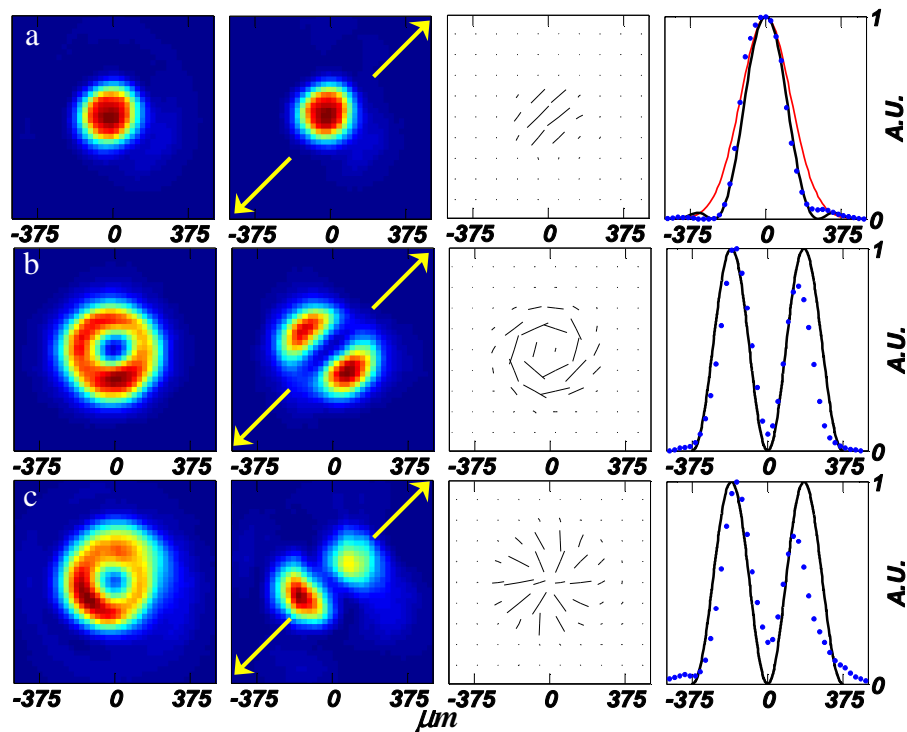
Fig. 8. (color online) Measured intensity and polarization for the inverse coupling and transformation of the TE$_{01}$ mode to: (a) a linearly polarized beam by use of PBOE with $n=0$ (red line shows the focus of a Gaussian beam having a similar width.), (b) a radially polarized beam by use of PBOE with $n=1$. (c) Azimuthally polarized beam obtained without a second PBOE. The first to fourth columns depicts the intensity, intensity after a polarizer (arrows indicate polarizer orientation), measured polarization orientation, and intensity cross-section (dots-measured, solid line-predicted), respectively.

4. Conclusions

We have proposed PBOEs as an efficient means of obtaining the space-variant polarization state of a waveguide mode, thereby enabling its efficient coupling to high order waveguide modes. We have experimentally demonstrated the coupling of linearly polarized light at a wavelength of $10.6\mu m$ to single vectorial modes of various orders within a hollow metallic waveguide by use of PBOEs. In addition, we demonstrated inverse transformation of the

fundamental low order TE_{01} mode to linearly and radially polarized free space modes. In a similar manner, any waveguide vectorial mode can be excited by a properly designed PBOE.